





Cite this article as: Hut T, Roest A, Gaillard D, Hazekamp M, van den Boogaard P, Lamb H *et al.* Virtual surgery to predict optimized conduit size for adult Fontan patients with 16-mm conduits. *Interdiscip CardioVasc Thorac Surg* 2023; doi:10.1093/icvts/ivad126.

Virtual surgery to predict optimized conduit size for adult Fontan patients with 16-mm conduits

Tjerry Hut^a, Arno Roest^b, Duco Gaillard^a, Mark Hazekamp^c, Pieter van den Boogaard^d, Hildo Lamb ^d, Lucia Kroft^d, Monique Jongbloed ^e, Jos Westenberg ^d, Jolanda Wentzel^f, Friso Rijnberg ^{c,*†} and Sasa Kenjeres^{a,†}

^a Department of Chemical Engineering, Faculty of Applied Sciences, Delft University of Technology and J.M. Burgers Centrum Research School for Fluid Mechanics, Delft, Netherlands

^b Department of Pediatric Cardiology, Leiden University Medical Center, Leiden, Netherlands

^c Department of Cardiothoracic Surgery, Leiden University Medical Center, Leiden, Netherlands

^d Department of Radiology, Leiden University Medical Center, Leiden, Netherlands

^e Department of Cardiology and Anatomy & Embryology, Leiden University Medical Center, Leiden, Netherlands

^f Department of Cardiology, Biomechanical Engineering, Erasmus MC, Rotterdam, Netherlands

* Corresponding author. Department of Cardiothoracic Surgery, Leiden University Medical Center, Albinusdreef 2, 2333 ZA Leiden, Netherlands. Tel: +31-715262348; e-mail: f.m.rijnberg@lumc.nl (F. Rijnberg).

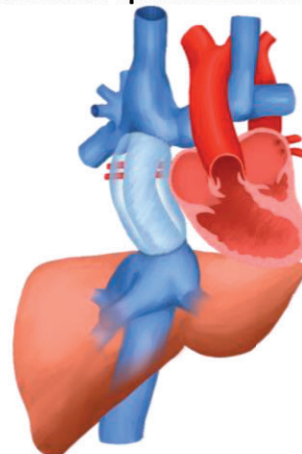
Received 25 March 2023; received in revised form 18 June 2023; accepted 30 July 2023

Virtual surgery to predict optimized conduit size for adult Fontan patients with 16mm conduits

Summary

This computational fluid dynamics study investigated the virtual implantation of 24–32mm conduits in 5 adult Fontan patients with 16mm conduits. Virtual conduit replacement led to a 40–65% decrease in pressure gradient across the total cavopulmonary connection, but the pulmonary arteries remained a significant residual source of increased energy losses.

40–65% improvement in hemodynamics after virtual conduit replacement to 24–32mm



Legend: Visualisation of the Fontan circulation with the virtual surgery to widen the conduit.

†The last two authors shared senior authorship.
Presented at the EACTS, Milan, Italy, 6th October, 2022.

Abstract

OBJECTIVES: Recent evidence suggests that conduits implanted in Fontan patients at the age of 2–4 years become undersized for adulthood. The objective of this study is to use computational fluid dynamic models to evaluate the effect of virtual expansion of the Fontan conduit on haemodynamics and energetics of the total cavopulmonary connection (TCPC) under resting conditions and increased flow conditions.

METHODS: Patient-specific, magnetic resonance imaging-based simulation models of the TCPC were performed during resting and increased flow conditions. The original 16-mm conduits were virtually enlarged to 3 new sizes. The proposed conduit sizes were defined based on magnetic resonance imaging-derived conduit flow in each patient. Flow efficiency was evaluated based on power loss, pressure drop and resistance and thrombosis risk was based on flow stagnation volume and relative residence time (RRT).

RESULTS: Models of 5 adult patients with a 16-mm extracardiac Fontan connection were simulated and subsequently virtually expanded to 24–32 mm depending on patient-specific conduit flow. Virtual expansion led to a 40–65% decrease in pressure gradient across the TCPC depending on virtual conduit size. Despite improved energetics of the entire TCPC, the pulmonary arteries remained a significant contributor to energy loss (60–73% of total loss) even after virtual surgery. Flow stagnation volume inside the virtual conduit and surface area in case of elevated RRT (>20/Pa) increased after conduit enlargement but remained negligible (flow stagnation <2% of conduit volume in rest, <0.5% with exercise and elevated RRT <3% in rest, <1% with exercise).

CONCLUSIONS: Virtual expansion of 16-mm conduits to 24–32 mm, depending on patient-specific conduit flow, in Fontan patients significantly improves TCPC efficiency while thrombosis risk presumably remains low.

Keywords: Univentricular heart disease • Fontan circulation • Computational fluid dynamics • Extracardiac conduit • Total cavopulmonary connection • Energy loss

ABBREVIATIONS

CSA	Cross-sectional area
ECG	Electrocardiogram
HV	Hepatic vein
IVC	Inferior vena cava
MRI	Magnetic resonance imaging
OSI	Oscillatory Shear Index
PA	Pulmonary artery
RRT	Relative residence time
SVC	Superior vena cava
TAWSS	Time-averaged wall shear stress
TCPC	Total cavopulmonary connection
VDR	Viscous dissipation rate

INTRODUCTION

In patients with a univentricular heart defect, the Fontan procedure directly connects the inferior vena cava (IVC) and superior vena cava (SVC) to the pulmonary arteries (PAs), resulting in the total cavopulmonary connection (TCPC). Most centres complete the TCPC at 2–4 years of age using the extracardiac conduit technique that connects the IVC to the PA using a 16- to 20-mm Goretex conduit that lacks growth potential [1].

Recent research indicates that these 16- to 20-mm extracardiac conduits become relatively undersized later in life [2], as important increases in velocity are observed at the level of the conduit. An undersized conduit results in inefficient blood flow with elevated energy losses and associated pressure drops across the TCPC [3]. Importantly, adverse TCPC flow efficiency has been linked to liver fibrosis in Fontan patients and a reduced exercise capacity [4, 5]. Improving flow conditions and minimizing energy loss in the TCPC are thus important goals and TCPC efficiency may be improved with larger conduits. However, larger conduits may increase the risk of conduit thrombosis caused by an IVC-conduit size mismatch and blood stasis [6, 7]. This necessitates

finding an optimal conduit size at adult age which leads to low energy losses and pressure drops without increased thrombosis risks.

Optimal conduit size will be patient specific and depends on the amount of conduit flow, which is highly variable between adult Fontan patients [2]. Based on a previous computational fluid dynamics (CFD) study in 51 patients, favourable pressure gradients ≤ 1.0 mmHg across the TCPC were present in rest and simulated exercise in patients with a functional conduit cross-sectional area (CSA in mm^2 normalized for conduit flow in l/min) of $\geq 125 \text{ mm}^2/\text{l/min}$ [8]. Therefore, the aim of the present study is to determine the impact of conduit expansion on TCPC pressure gradients and thrombosis risk markers using CFD models with virtual surgery. The main goal is to find optimized conduit sizes for adult Fontan patients. We hypothesize that larger conduits perform considerably better, improving the efficiency of the TCPC without instigating thrombus development.

PATIENTS AND METHODS

Ethical statement

The study was approved by the medical ethical review committee of the hospital (P18.024). Written informed consent was obtained from all patients and/or their parents.

Study population

Fontan patients were evaluated using a comprehensive cardiovascular magnetic resonance imaging (MRI) protocol between 2018 and 2021 at the Leiden University Medical Center as part of a previous prospective study [9]. All patients >8 years old without contraindications for MRI were eligible for inclusion. In the present study, a subset of adult Fontan patients with a 16-mm conduit were selected from a previously published cohort of 51 patients who underwent CFD analysis of the TCPC haemodynamics [8]. Selection was based on conduit flow, with the goal to

include the full range of different conduit flow rates observed in adult Fontan patients. Selected patients were 17–22 years old and all underwent previous Fontan completion using a 16-mm extracardiac Goretex conduit, which was the conduit size of choice at that time in our institution.

Magnetic resonance imaging

Patient blood flow rates were measured in the SVC, left pulmonary artery (LPA), right pulmonary artery (RPA), subhepatic IVC (before hepatic veins enter) and inside the conduit. Flow in the conduit, SVC and subhepatic IVC was measured with real-time 2D flow MRI on a 3-T scanner (Philips Healthcare), consisting of 250 flow measurements without electrocardiogram (ECG) gating while monitoring the respiratory signal using an abdominal belt filled with air. Mean flow rates were determined from 2 to 4 consecutive respiratory cycles as previously described [2]. At the PAs, only free-breathing 2D ECG-gated flow MRI measurements were performed. Hepatic vein (HV) flow was derived as the difference between conduit and subhepatic IVC flow. No patient had a patent fenestration. Flow rate at each vessel was acquired by manual segmentation of the vessel lumen on all phase-contrast images (Mass software, Leiden, Netherlands). The detailed methodology is described in a previous study [2].

Geometry preparation

Patient-specific three-dimensional geometries of the TCPC were created from sagittal and transversal 2D anatomical stacks (5-mm slices, 2.5-mm overlap, reconstructed resolution $0.9\text{ mm} \times 0.9\text{ mm}$) [10]. Included were the subhepatic IVC, HVs, SVC and RPA (including the right upper lobe branches) and LPA up to the segmental branches (ITK-SNAP). After smoothing the geometry, flow extensions ($3 \times$ diameter) were added at the in- and outlets using the Vascular Modelling Toolkit [11]. Reported conduit diameters were determined as the mean value of 1-mm interval measurements perpendicular to the centreline. The presurgery geometries are shown in [Supplementary Material S.1](#).

Virtual surgery was performed by adopting the following procedure: (i) the centreline of the original geometry is extracted

(Vascular Modelling Toolkit and NeuroMorph toolset in Blender v2.93.1, Amsterdam, Netherlands); (ii) the start and the end of the conduit are specified (Blender); (iii) this subdomain is then replaced with a cylindrical-shape conduit of the new desired size around the extracted nodes (Blender); and (iv) a smooth transition between the conduit and the rest of geometry is manually created (Autodesk Meshmixer v3.5.474, Inc., San Rafael, CA, USA).

Three new TCPC models with expanded conduit diameters were created: (i) a TCPC with a desirable diameter ($125\text{ mm}^2/\text{l/min}$, rounded to the closest clinically available size), (ii) a conduit 2 sizes larger (i.e. 4-mm diameter) and (iii) a conduit 2 sizes smaller. Expanded conduits followed the original centreline exactly and smoothing was performed manually to ensure a smooth transition between conduit and PAs/IVC. The virtual widening of 1 modelled patient (case 5) is visualized in Fig. 1.

Computational fluid dynamics

Polyhedral meshes were generated inside the geometries (ANSYS ICEM and ANSYS Fluent v19.1, Inc., Canonsburg, PA, USA). Respiratory cycle-resolved blood flow rate measurements were imposed at the inlets as parabolic velocity profiles (the inclusion of respiration effects is preferred when estimating power losses and thrombosis markers [12]). The total HV flow rate was subdivided over each HV based on the relative CSA. Pre-surgery outlet flow ratios at the PAs were determined based on ECG-gated 2D flow MRI measurements in the LPA branch and 1 RPA branch. A flow distribution according to Murray's law was used to divide the total RPA flow over the multiple RPA branches. Post-surgery outflow ratios were determined using a three-element Windkessel model based on the pre-surgical simulations (described in [Supplementary Material S.2](#)). The walls of the geometry were considered rigid with no-slip boundaries. Density was assumed constant (1060 kg/m^3). Blood viscosity was simulated using the non-Newtonian Carreau model and computed as laminar [13]. One respiratory cycle was simulated to initialize the velocity field, and the second cycle was used for data analysis. Every cycle was divided into 5000 equally spaced time steps.

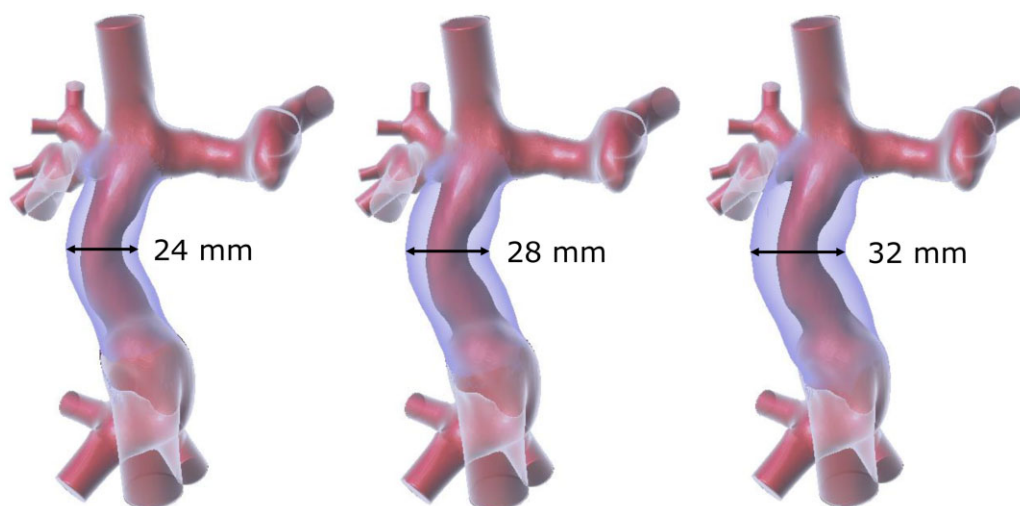


Figure 1: Visualisation of the 3 different virtual surgeries performed on case 5, with the red geometry describing the original total cavopulmonary connection and the blue overlay denoting the resulting width after virtual surgery.

Exercise conditions

To simulate the effect of increased flow during exercise on local TCPC haemodynamics, flow rates were increased based on a study by Wei *et al.* [14], which measured flow conditions before and after lower-leg exercise at the ventilatory threshold; total respiratory cycle length was decreased by 60%, IVC and HV flow rates were increased by 144% and SVC flow rates were increased by 67%. Lastly, in line with findings by Hjortdal *et al.* [15], relative inspiration time was increased by 17%.

Haemodynamic parameters

Energy loss. Local energy losses were calculated using the viscous dissipation rate (VDR) method [16]. The pressure drop (mmHg) inside the TCPC is calculated by dividing the total energy loss (mW) by the mean total blood flow. A normalized TCPC resistance (mmHg/l/min/m²) was then calculated, normalizing for patient body surface area (Haycock formula) [17]. All relevant equations are given below, where $\mathbf{u}(u_x, u_y, u_z)$ describe velocity components, Q_{tot} is the total blood flow and μ is the viscosity.

$$\text{VDR} = \mu \left[2 \left(\frac{\partial u_x}{\partial x} \right)^2 + 2 \left(\frac{\partial u_y}{\partial y} \right)^2 + 2 \left(\frac{\partial u_z}{\partial z} \right)^2 + \left(\frac{\partial u_x}{\partial y} + \frac{\partial u_y}{\partial x} \right)^2 + \left(\frac{\partial u_x}{\partial z} + \frac{\partial u_z}{\partial x} \right)^2 + \left(\frac{\partial u_y}{\partial z} + \frac{\partial u_z}{\partial y} \right)^2 \right]$$

$$\Delta P = \frac{\int \text{VDR}}{Q_{\text{tot}}}$$

$$\text{Normalized resistance} = \frac{\Delta P_{\text{TCPC}}}{\frac{Q_{\text{tot}}}{\text{BSA}}}$$

Mean VDR, pressure gradient and normalized resistance along the respiratory cycle were reported. To further determine the effects of conduit widening on local TCPC haemodynamics, the TCPC was separated into 3 regions: (i) conduit, (ii) above conduit (PAs and SVC) and (iii) below conduit (HVs and IVC). The VDR was determined for all regions separately.

Thrombosis markers. Thrombosis risk was estimated using 2 markers. First, flow stagnation was measured as the percentage of the volume with a velocity of <1 cm/s [7], measured during peak inspiration (highest flow) to reflect the area of possible long-term stasis. The assessment was performed for the entire TCPC, as well as for the conduit separately.

Second, the relative residence time (RRT) was calculated at the walls to capture irregular and unsteady flow behaviour. The RRT is a commonly used potential measurement for thrombosis risk in the human circulatory system [18]. The RRT is defined below, where the time-averaged wall shear stress (TAWSS) is the mean shear stress over a full respiratory cycle and the Oscillatory Shear Index (OSI) is a measurement of local flow direction. Both metrics were previously similarly used in Fontan patients as a marker for thrombosis [19]. The OSI is bounded between 0 and 0.5, where 0 describes flow that is entirely unidirectional and 0.5 describes flow with no average direction.

$$\text{RRT} = \frac{1}{\text{TAWSS}(1 - 2 \times \text{OSI})}$$

$$\text{TAWSS} = \frac{1}{T} \int_0^T |\tau_w| dt = \frac{1}{T} \int_0^T \left| \mu(\dot{\gamma}) \frac{du_i}{dx_j} \right|_{\text{Wall}} dt$$

where τ_w is the wall shear stress.

$$\text{OSI} = \frac{1}{2} \left(1 - \frac{\left| \int_0^T \tau_w dt \right|}{\int_0^T |\tau_w| dt} \right)$$

Thrombosis risk elevation will be estimated based on a risk threshold. Grande Gutierrez *et al.* [20] found, for children with Kawasaki disease, that thrombosis had developed in regions with a TAWSS of <0.1 Pa and an OSI of >0.25. Using these thresholds, the defined threshold for the RRT is 20/Pa.

Statistical analysis

Data were presented as median (Q1–Q3). A pairwise comparison of parameters between the original conduit size and the virtually enlarged conduit sizes were performed using the Friedman test. A *P*-value of <0.05 was considered statistically significant. Data were analysed with SPSS 25.0 (IBM Corp., Armonk, NY, USA).

RESULTS

Five adult Fontan patients with a 16-mm conduit were included in this study. All patients were in NYHA class I and II. Mean conduit flow rates along the respiratory cycle in selected patients ranged between 2.2 and 4.8 l/min. Projected conduit diameters of ± 125 mm²/l/min ranged from 20 to 28 mm. Patient characteristics are presented in Table 1.

Power loss

Mean power loss, pressure drop and normalized resistance along the respiratory cycle of the original TCPCs and all virtual surgery models are reported in Tables 2 and 3, including the relative improvement in energetics compared to presurgery.

At rest, power loss in TCPCs including conduits sized for ± 125 mm²/l/min decreased by 38–55% (median 41%, Q1–Q3 38.5–53.5%) compared to the original [median power loss 8.2 (Q1–Q3 3.5–14.5 mW) and 3.9 (Q1–Q3 1.9–8.7 mW), *P*=0.014]. Absolute power losses and pressure gradients showed a strong correlation (ρ =0.97–0.98, *P*<0.001) and were highest in patients with the highest flow rates. Power loss increased ~4- to 6-fold during exercise conditions but did not affect relative improvement (median 43%, Q1–Q3 38.5–56.5%, *P*=0.39). In all cases, implantation of the largest conduits (range 24–32 mm) further decreased power loss (median 58%, Q1–Q3 48–61% in rest and 60%, Q1–Q3 47.5–65% with exercise) compared to original [median power loss 58.0 (Q1–Q3 23.8–99.4 mW) and 26.2 (Q1–Q3 12.2–60.3 mW), *P*<0.001]. Power loss inside the TCPC is visualized for all simulated versions of case 3 as a typical example (Fig. 2).

Table 1: Patient characteristics

Patient	Age (years)	Implanted conduit diameter (mm)	Measured conduit diameter (mm)	Flow (l/min)	BSA (m ²)	Desirable diameter (i.e. 125 mm ² /l/min) (mm)	Simulated diameters (mm)
1	17.4	16	14.5	2.2	1.69	18.9	18–20–24
2	21.3	16	16.0	3.0	1.67	21.9	18–22–26
3	18.2	16	16.2	3.8	1.74	24.6	20–24–28
4	22.2	16	15.5	4.4	1.76	26.5	22–26–30
5	22.8	16	15.8	4.8	2.04	27.6	24–28–32

Table 2: Mean power loss, pressure drop and normalized resistance along the respiratory cycle and the relative improvement compared to presurgery in rest

Patient	Conduit diameter (mm)	Functional conduit size (mm ² /l/min)	Power loss (mW)	Relative improvement (%)	Pressure drop (mmHg)	Norm. resist. (mmHg/l/min/m ²)
1	14.5 (original)	75	3.2	–	0.49	0.28
	18	116	1.6	48	0.25	0.15
	20	143	1.4	55	0.22	0.13
	24	206	1.2	61	0.19	0.11
2	16.0 (original)	67	3.7	–	0.43	0.18
	18	85	2.7	26	0.31	0.13
	22	127	2.3	38	0.26	0.11
	26	177	1.9	49	0.21	0.09
3	16.2 (original)	54	8.3	–	0.80	0.30
	20	83	5.1	38	0.49	0.18
	24	119	3.9	52	0.38	0.14
	28	162	3.3	61	0.31	0.12
4	15.5 (original)	43	12.1	–	0.86	0.24
	22	86	7.8	35	0.56	0.16
	26	121	7.1	41	0.51	0.14
	30	161	5.0	58	0.36	0.10
5	15.8 (original)	41	16.9	–	1.28	0.44
	24	94	10.7	37	0.81	0.28
	28	128	10.2	39	0.78	0.27
	32	168	8.9	47	0.68	0.23

Table 3: Mean power loss, pressure drop and normalized resistance along the respiratory cycle and the relative improvement compared to presurgery with simulated exercise

Case	Conduit diameter (mm)	Power loss (mW)	Relative improvement (%)	Pressure drop (mmHg)	Norm. resist. (mmHg/l/min/m ²)
1	14.5 (original)	21.6	–	1.43	0.36
	18	10.8	50	0.71	0.18
	20	9.0	58	0.60	0.15
	24	7.5	65	0.50	0.12
2	16.0 (original)	25.9	–	1.27	0.23
	18	19.8	24	0.97	0.18
	22	15.3	41	0.75	0.14
	26	11.9	54	0.58	0.11
3	16.2 (original)	58.0	–	2.36	0.37
	20	36.7	37	1.49	0.23
	24	26.2	55	1.06	0.17
	28	20.4	65	0.83	0.13
4	15.5 (original)	88.4	–	2.76	0.34
	22	54.2	39	1.69	0.21
	26	50.3	43	1.57	0.19
	30	35.3	60	1.10	0.14
5	15.8 (original)	110.4	–	3.60	0.53
	24	75.4	32	2.46	0.36
	28	70.2	36	2.29	0.34
	32	65.3	41	2.13	0.32

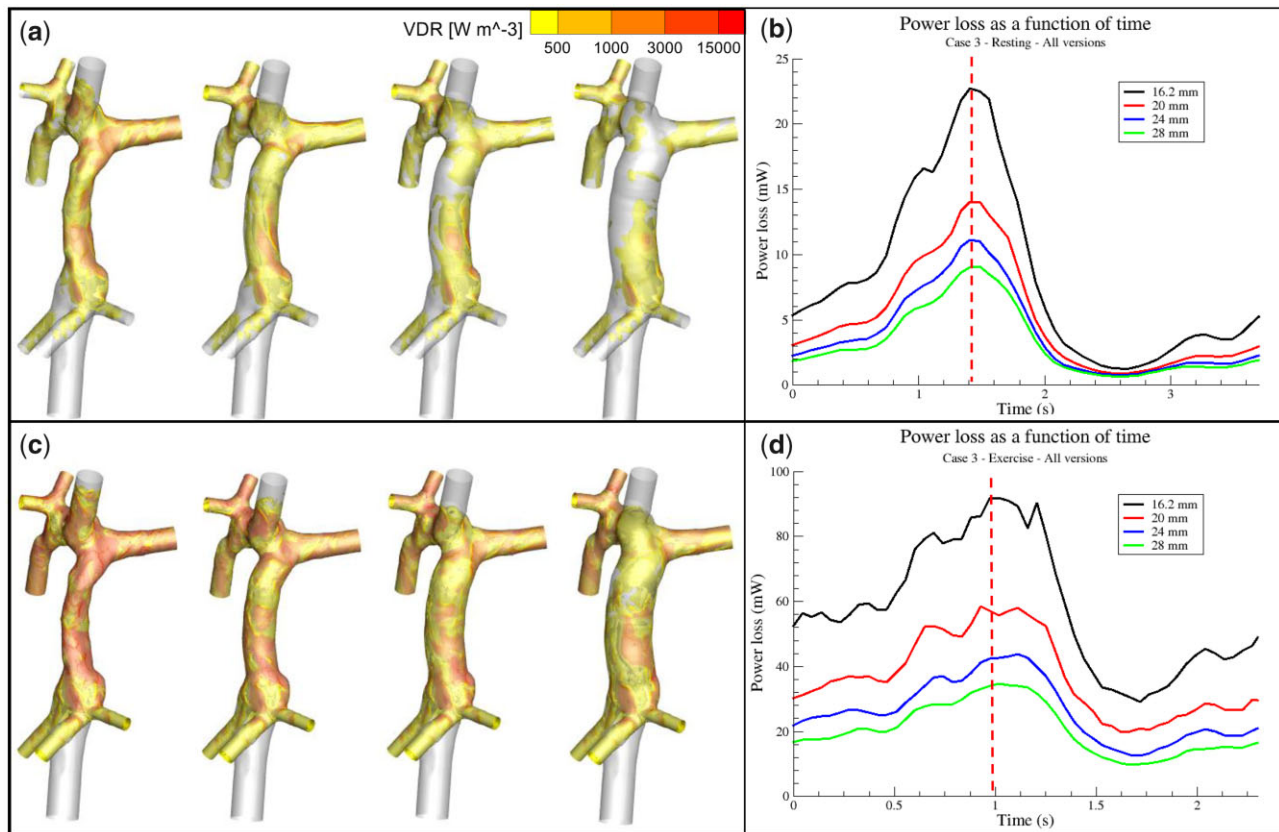


Figure 2: Wall contours of local viscous dissipation rate visualizing regions of high power loss (**A** and **C**), also denoted by the dotted red line in the time-dependent results (**B** and **D**). Similar regions of high local power loss gradually disappear in both resting (A+B) and with exercise (C+D).

Segmental power losses. The segmental assessment of TCPC energetics is reported in Fig. 3. Percentual distribution of energy losses between segments was not significantly different between rest and exercise in all simulations ($P=0.50$ to $P=0.69$), the described data in this section will only be based on resting conditions.

Before surgery, the region below the conduit constitutes 8% (Q1–Q3 6–11%), the conduit 24% (Q1–Q3 21–29%) and the region above the conduit 68% (Q1–Q3 60–73%) of the total power loss. After virtual expansion to ± 125 mm²/l/min conduits size, absolute energy loss of the entire TCPC decreased but the division remained similar although reaching statistical significance: 12% (Q1–Q3 10–20%, $P=0.043$), 19% (Q1–Q3 11–24%, $P=0.043$) and 68% (Q1–Q3 56–78%, $P=0.50$). In ± 125 mm²/l/min conduits, energy loss inside the conduit decreased by a median of 62% from 2.5 mW (Q1–Q3 0.9–3.1 mW) to 0.7 mW (Q1–Q3 0.3–1.3 mW, $P=0.014$). The largest contributor, the region above the conduit, decreased a median of 45% from 4.6 mW (Q1–Q3 2.3–8.4 mW) to 1.8 mW (Q1–Q3 1.3–6.7 mW, $P=0.014$).

Thrombosis risk factors

Blood stasis. Flow stagnation volume in the entire TCPC and in the conduit is reported in Figs 4 and 5. Flow stagnation inside the entire TCPC increased minimally after the implantation of larger conduits. In rest, the total flow stagnation in the entire TCPC pre-surgery (median 1.15%, Q1–Q3 0.9–1.9%) was not significantly different after implantation of conduits of ± 125 mm²/l/min (median 1.21%, Q1–Q3 1.0–2.0%, $P=0.46$) (Fig. 4). Flow stagnation in the

conduit increased from a median of 0.06% (Q1–Q3 0.035–0.24%) to 0.31% (Q1–Q3 0.20–0.56%, $P=0.68$). Even in the largest implanted conduits, flow stagnation volume remained negligible (median 0.63% of the conduit in rest). The largest flow stagnation volume in the conduit was measured at <1.5% in case 1 (Fig. 5). During exercise, flow stagnation in the total geometry and conduit decreased further in all modelled cases ($P=0.001$ to $P=0.03$).

Relative residence time. The percentage of the wall surface that exceeded the RRT of >20 /Pa threshold was determined in Fig. 6. In resting conditions, <2% of the total TCPC wall surface pre-surgery (median 0.6%, Q1–Q3 0.4–1.3%) revealed elevated RRT. Compared to the original conduit size, conduits sized for ± 125 mm²/l/min showed no significantly different percentage of elevated RRT (median 0.9%, Q1–Q3 0.5–1.5%, $P=0.05$) but significantly increased in the largest conduits modelled (median 1.5%, Q1–Q3 0.7–2.2%, $P=0.001$). During exercise conditions, <1% of the surface area exceeded the threshold and the complete group of post-surgery conduits showed no increased elevation of the RRT compared to the original conduit (median 0.12%, Q1–Q3 0.06–0.27% before surgery, 0.15%, Q1–Q3 0.1–0.25% after surgery, $P=0.08$).

DISCUSSION

The relative undersizing of 16-mm conduits for adult Fontan patients leads to suboptimal flow conditions and haemodynamics [2]. In the current study, virtual implantation of larger

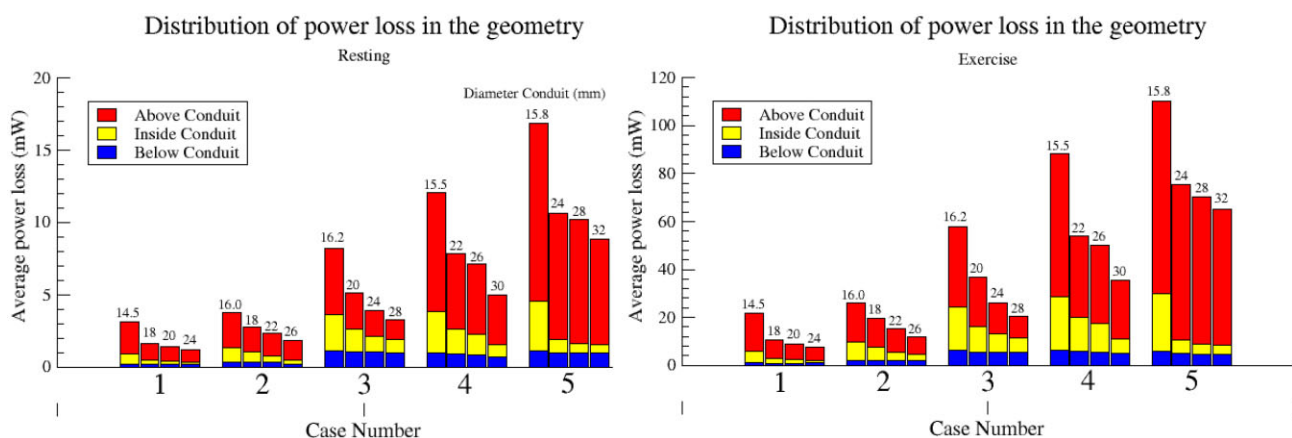


Figure 3: The distribution of power loss in the simulated total cavopulmonary connection geometries separated as 'above conduit' in red, 'inside conduit' in yellow and 'below conduit' (inferior vena cava) in blue. Numbers above the bar graph describe the simulated width of the conduit in millimetres.

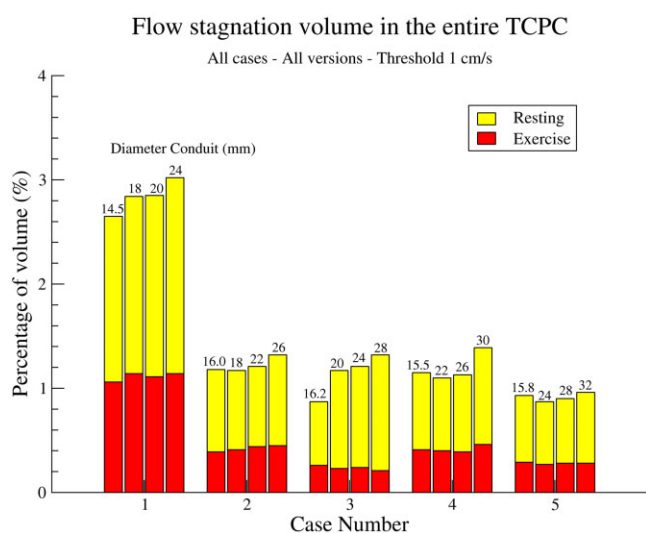


Figure 4: The flow stagnation volume during peak inspiration in rest (yellow) and after increasing flow with simulated exercise (red) in the entire total cavopulmonary connection in all simulated geometries is shown. Numbers above the bar graph describe the simulated width of the conduit in millimetres.

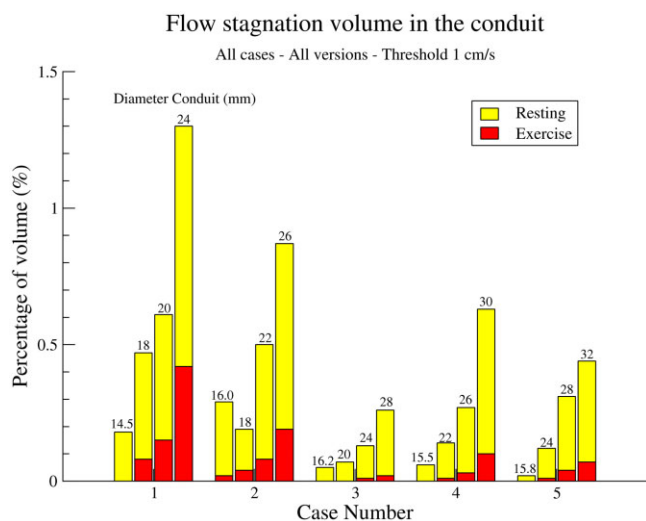


Figure 5: The flow stagnation volume during peak inspiration in the conduit in rest (yellow) and increasing flow with simulated exercise (red) in all simulated geometries is shown. Numbers above the bar graph describe the simulated width of the conduit in millimetres.

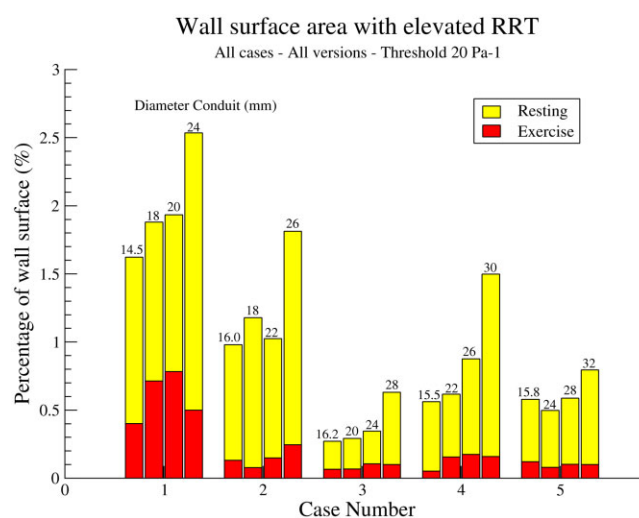


Figure 6: The wall surface area with elevated relative residence time ($>20/\text{Pa}$) of the total cavopulmonary connection in rest (yellow) and increasing flow with simulated exercise (red) in all simulated geometries. Averaged over 1 full respiratory cycle. Numbers above the bar graph describe the simulated width of the conduit in millimetres.

extracardiac conduits showed that pressure gradients inside the TCPC can be reduced with 40–65% by implanting 24–32mm conduits, without considerably elevating thrombosis risk markers. Ideal conduit sizes depend on patient-specific conduit flow rate. Power loss in the PAs decreased with virtual enlargement of the conduit but remained the most dominant region of power loss within the TCPC, emphasizing the importance of optimization of PA size on TCPC efficiency.

Conduit design and power loss

Strong blood flow accelerations in the Fontan circulation were previously found between the IVC and conduit in adolescent patients, showing relative undersizing of the conduit compared to its surrounding vessels [2, 21]. The discrepancy between the size of these vessels was investigated, and a correlation was found between conduit size and energy loss leading to a decrease in TCPC efficiency [3]. Subsequently, reduced TCPC efficiency has been related to elevated levels of liver fibrosis [5], as well as to a

reduced exercise capacity [8, 22], further emphasizing the importance of proper conduit sizing.

The performed virtual surgery further exemplifies the importance of adequate conduit sizing, especially for adulthood. The 16- to 18-mm conduits may be adequate sizes for children [7], but larger widths performed vastly better in the current study in adult patients with different conduit flow rates. Virtual enlargement of 16-mm conduits to 24- to 26-mm conduits considerably improved haemodynamics and were shown to be suitable fits in patients with conduit flow rates ≤ 3.0 l/min (functional conduit size 177–206 mm²/l/min in rest). In patients with flow rates > 3.0 l/min, conduits sized 28–32 mm performed well (161–168 mm²/l/min). These conduit diameters are in agreement with the expected size of the suprahepatic IVC in healthy adults and with diameters of lateral tunnel patients [23, 24]. This study thus emphasizes that standardized 16- to 20-mm conduits, which are sufficient at the age of Fontan completion, are suboptimal for a large portion of adult Fontan patients and that diameters up to 28–32 mm may be preferable in large adults with high conduit flow instead.

Importantly, optimization of the Fontan circulation does not depend solely on the implanted conduit. The relatively simple, cylindrical shape of the conduit does not necessarily promote the loss of energy as considerably as the PAs do. The direct mixing of blood flow from the conduit and SVC, just above the conduit, followed by the sharp rerouting into the PAs is a considerable source of local flow disruption. Furthermore, stenosis in the PAs leads to increased energy losses [3] and is correlated to reduced exercise capacity [22]. Therefore, the presence of PA stenosis or hypoplasia promotes the loss of energy inside the Fontan circulation emphasizing the importance of also adequately sized PAs. Absolute power loss in the PAs decreased with the virtual enlargement of the conduit but remained the most dominant region of power loss within the TCPC. Further improvement in TCPC efficiency can therefore be expected with intervention to the PAs, which could include dilatation of the PAs or exclusion of a dilated pulmonary trunk when present [25]. These findings do, however, also show that properly sized conduits decrease flow disruption and reduce energy losses further downstream. As a result, conduit sizing does not only affect energy loss inside the conduit but also affects the TCPC efficiency downstream.

Thrombosis risks

Elevated thrombosis risks compared to healthy persons are a potential source of morbidity of the Fontan circulation. Stagnant and irregular blood flow profiles promote these risks and thrombosis has previously formed in oversized conduits implanted in young children [26]. In children around 3 years old, stagnation volume with 20-mm conduits could reach up to 30% [7]. In our study, the stagnation volume increased in larger conduits but never exceeded 2% of the total volume. The increased thrombosis risk potential appears therefore negligible in these conduits, where their cylindrical shape promotes organized flow conditions. The RRT analysis confirms this by not showing significantly elevated recirculation in the expanded conduits. Thus, no evidence was found of adverse effects resulting from the virtual expansion.

Clinical relevance for surgical strategy

Due to anatomical and physiological limitations during initial Fontan completion (as patients are only 2–4 years of age), the implantation of larger conduits is not possible or desirable as significant oversizing may promote thrombosis development in early life [7, 26]. A standard Fontan tunnel may only stay adequately sized for all ages if it has elastic properties or otherwise enables conduit expansion, emphasizing the important future potential of using dilatable conduits. The current study showcases the necessity of researching such novel materials, including the amount of expansion that is clinically feasible. Other options include stenting of the existing Fontan conduit, which not only can be used in cases of conduit stenosis but also allows for expansion of unobstructed but undersized conduits with up to 127–165% of original [27]. However, such increases are much lower compared to the increases modelled in our study (up to 3–4 times increase in CSA of the conduit).

Limitations

This study describes the results of only 5 Fontan patients, making statistical analyses and generalizations difficult. Another limitation is the usage of simulated exercise using cohort-averaged data. Patient-specific exercise data would have shown the differences between resting and exercise more accurately, though the interactions between flow rate and local TCPC performance markers are unaffected by the loss of specificity. A small discrepancy between simulated and real patients can be expected resulting from the ECG-gated data used for the outlet boundary conditions, and used thresholds (1 mmHg pressure drop, velocity < 1 cm/s, RRT > 20 /Pa) are merely estimations, as strong data linking specific thresholds to thrombosis formation are lacking. Lastly, the investigated virtual surgeries do not necessarily match real surgical interventions. The effects of physical and anatomical limitations on virtual conduit enlargement (e.g. pulmonary vein compression) were not explored.

CONCLUSIONS

CFD simulations suggest that extracardiac Fontan conduits with a 16-mm width are structurally undersized for adult patients, leading to elevated pressure drops and resistances inside the Fontan circulation.

After virtual implantation of larger conduits of 22–32 mm, TCPC efficiency improved with 40–65% while thrombosis risk markers increased only minimally. The region downstream of the conduit (pulmonary arteries) was the most significant source of energy loss. Virtual expansion not only decreased energy loss inside the conduit but also successfully improved TCPC efficiency in the region downstream of the conduit.

In conclusion, computational fluid dynamic modelling suggests that suboptimal TCPC energetics in adult patients with 16-mm conduits can be improved with larger conduits. The use of dilatable conduits for the completion of the Fontan procedure should be explored.

SUPPLEMENTARY MATERIAL

Supplementary material is available at *ICVTS* online.

ACKNOWLEDGEMENTS

We acknowledge Kyra S. McCannell for designing the illustration in the graphical abstract and Rosemary Bolt and Martijn de Vlieger for developing a proof of concept of the virtual surgery.

Funding

This work was supported by the Dutch Heart Foundation [2018-T083 to Friso Rijnberg], Stichting Hartekind [to Friso Rijnberg] and the Dutch national e-infrastructure with the support of the SURF Cooperative [EINF-3030].

Conflict of interest: none declared.

DATA AVAILABILITY

The data underlying this article will be shared on reasonable request to the corresponding author.

Author contributions

Tjerry Hut: Conceptualization; Formal analysis; Investigation; Visualization; Writing—original draft. **Arno Roest:** Conceptualization; Investigation; Supervision; Writing—review & editing. **Duco Gaillard:** Methodology; Writing—review & editing. **Mark Hazekamp:** Writing—review & editing. **Pieter van den Boogaard:** Data curation; Writing—review & editing. **Hildo Lamb:** Resources; Writing—review & editing. **Lucia Kroft:** Resources; Writing—review & editing. **Monique Jongbloed:** Writing—review & editing. **Jos Westenberg:** Data curation; Resources; Writing—review & editing. **Jolanda Wentzel:** Investigation; Writing—review & editing. **Friso Rijnberg:** Conceptualization; Data curation; Funding acquisition; Investigation; Writing—review & editing. **Sasa Kenjeres:** Conceptualization; Formal analysis; Investigation; Methodology; Supervision; Writing—review & editing.

Reviewer information

Interdisciplinary CardioVascular and Thoracic Surgery thanks Hans-Heiner Kramer, Katrien Francois and the other anonymous reviewer(s) for their contribution to the peer review process of this article.

REFERENCES

- [1] Rychik J, Atz AM, Celermajer DS, Deal BJ, Gatzoulis MA, Gewillig MH *et al.*; American Heart Association Council on Cardiovascular Disease in the Young and Council on Cardiovascular and Stroke Nursing. Evaluation and management of the child and adult with Fontan circulation: a scientific statement from the American Heart Association. *Circulation* 2019;140(6): e234–e284.
- [2] Rijnberg FM, van der Woude SFS, Hazekamp MG, van den Boogaard PJ, Lamb HJ, Terol Espinosa de Los Monteros C *et al.* Extracardiac conduit adequacy along the respiratory cycle in adolescent Fontan patients. *Eur J Cardiothorac Surg* 2022;62.
- [3] Tang E, Restrepo M, Haggerty CM, Mirabella L, Bethel J, Whitehead KK *et al.* Geometric characterization of patient-specific total cavopulmonary connections and its relationship to hemodynamics. *JACC Cardiovasc Imaging* 2014;7:215–24.
- [4] Lee SY, Song MK, Kim GB, Bae EJ, Kim SH, Jang SI *et al.* Relation between exercise capacity and extracardiac conduit size in patients with Fontan circulation. *Pediatr Cardiol* 2019;40:1584–90.
- [5] Trusty PM, Wei ZA, Rychik J, Graham A, Russo PA, Surrey LF *et al.* Cardiac magnetic resonance-derived metrics are predictive of liver fibrosis in Fontan patients. *Ann Thorac Surg* 2020;109:1904–11.
- [6] Firdouse M, Agarwal A, Chan AK, Mondal T. Thrombosis and thromboembolic complications in Fontan patients: a literature review. *Clin Appl Thromb Hemost* 2014;20:484–92.
- [7] Itatani K, Miyaji K, Tomoyasu T, Nakahata Y, Ohara K, Takamoto S *et al.* Optimal conduit size of the extracardiac Fontan operation based on energy loss and flow stagnation. *Ann Thorac Surg* 2009;88:565–72; discussion 72–3.
- [8] Rijnberg FM, van't Hul LC, Hazekamp MG, van den Boogaard PJ, Juffermans JF, Lamb HJ *et al.* Haemodynamic performance of 16–20-mm extracardiac Goretex conduits in adolescent Fontan patients at rest and during simulated exercise. *Eur J Cardiothorac Surg* 2022;63.
- [9] Rijnberg FM, Westenberg JJM, van Assen HC, Juffermans JF, Kroft LJM, van den Boogaard PJ *et al.* 4D flow cardiovascular magnetic resonance derived energetics in the Fontan circulation correlate with exercise capacity and CMR-derived liver fibrosis/congestion. *J Cardiovasc Magn Reson* 2022;24:21.
- [10] Rijnberg FM, van der Woude SFS, van Assen HC, Juffermans JF, Hazekamp MG, Jongbloed MRM *et al.* Non-uniform mixing of hepatic venous flow and inferior vena cava flow in the Fontan conduit. *J R Soc Interface* 2021;18:20201027.
- [11] Antiga L, Piccinelli M, Botti L, Ene-Iordache B, Remuzzi A, Steinman DA. An image-based modeling framework for patient-specific computational hemodynamics. *Med Biol Eng Comput* 2008;46:1097–112.
- [12] van der Woude SFS, Rijnberg FM, Hazekamp MG, Jongbloed MRM, Kenjeres S, Lamb HJ *et al.* The influence of respiration on blood flow in the Fontan circulation: insights for imaging-based clinical evaluation of the total cavopulmonary connection. *Front Cardiovasc Med* 2021;8: 683849.
- [13] Seo T, Schachter LG, Barakat AI. Computational study of fluid mechanical disturbance induced by endovascular stents. *Ann Biomed Eng* 2005; 33:444–56.
- [14] Wei Z, Whitehead KK, Khiabani RH, Tree M, Tang E, Paridon SM *et al.* Respiratory effects on Fontan circulation during rest and exercise using real-time cardiac magnetic resonance imaging. *Ann Thorac Surg* 2016; 101:1818–25.
- [15] Hjortdal VE, Emmertsen K, Stenbog E, Frund T, Schmidt MR, Kromann O *et al.* Effects of exercise and respiration on blood flow in total cavopulmonary connection: a real-time magnetic resonance flow study. *Circulation* 2003;108:1227–31.
- [16] Wei ZA, Tree M, Trusty PM, Wu W, Singh-Gryzbon S, Yoganathan A. The advantages of viscous dissipation rate over simplified power loss as a Fontan hemodynamic metric. *Ann Biomed Eng* 2018;46: 404–16.
- [17] Haggerty CM, Restrepo M, Tang E, de Zelicourt DA, Sundareswaran KS, Mirabella L *et al.* Fontan hemodynamics from 100 patient-specific cardiac magnetic resonance studies: a computational fluid dynamics analysis. *J Thorac Cardiovasc Surg* 2014;148:1481–9.
- [18] Dueñas-Pamplona J, García JG, Sierra-Pallares J, Ferrera C, Agujetas R, López-Mínguez JR. A comprehensive comparison of various patient-specific CFD models of the left atrium for atrial fibrillation patients. *Comput Biol Med* 2021;133:104423.
- [19] Schwarz EL, Kelly JM, Blum KM, Hor KN, Yates AR, Zbinden JC *et al.* Hemodynamic performance of tissue-engineered vascular grafts in Fontan patients. *NPJ Regen Med* 2021;6:38.
- [20] Grande Gutierrez N, Mathew M, McCrindle BW, Tran JS, Kahn AM, Burns JC *et al.* Hemodynamic variables in aneurysms are associated with thrombotic risk in children with Kawasaki disease. *Int J Cardiol* 2019;281: 15–21.
- [21] Rijnberg FM, Elbaz MSM, Westenberg JJM, Kamphuis VP, Helbing WA, Kroft LJ *et al.* Four-dimensional flow magnetic resonance imaging-derived blood flow energetics of the inferior vena cava-to-extracardiac conduit junction in Fontan patients. *Eur J Cardiothorac Surg* 2019;55: 1202–10.

- [22] Khiabani RH, Whitehead KK, Han D, Restrepo M, Tang E, Bethel J *et al.* Exercise capacity in single-ventricle patients after Fontan correlates with haemodynamic energy loss in TCPC. *Heart* 2015;101:139-43.
- [23] Ettinger E, Steinberg I. Angiocardigraphic measurement of the cardiac segment of the inferior vena cava in health and in cardiovascular disease. *Circulation* 1962;26:508-15.
- [24] Restrepo M, Mirabella L, Tang E, Haggerty CM, Khiabani RH, Fynn-Thompson F *et al.* Fontan pathway growth: a quantitative evaluation of lateral tunnel and extracardiac cavopulmonary connections using serial cardiac magnetic resonance. *Ann Thorac Surg* 2014;97:916-22.
- [25] Rijnberg FM, van Assen HC, Hazekamp MG, Roest AAW. Tornado-like flow in the Fontan circulation: insights from quantification and visualization of viscous energy loss rate using 4D flow MRI. *Eur Heart J* 2019;40:2170.
- [26] Alexi-Meskishvili V, Ovrouski S, Ewert P, Dahnert I, Berger F, Lange PE *et al.* Optimal conduit size for extracardiac Fontan operation. *Eur J Cardiothorac Surg* 2000;18:690-5.
- [27] Salaets T, Cools B, De Meester P, Heying R, Boshoff D, Eyskens B *et al.* Stent expansion of restrictive Fontan conduits to nominal diameter and beyond. *Catheter Cardiovasc Interv* 2022;100:1059-66.